Polarization-independent drop filters based on photonic crystal self-collimation ring resonators

Xiyao Chen[1,3], Zexuan Qiang[2,3], Deyin Zhao[3], Hui Li[2], Yishen Qiu[2], Weiquan Yang[3], and Weidong Zhou[3*]

[1]*Department of Physics and Electronic Information Engineering, Minjiang University, Fuzhou, 350108, P. R. China*
[2]*School of Physics and Optoelectronics Technology, Fujian Normal University, Fuzhou, 350007, P. R. China*
[3]*Department of Electrical Engineering, NanoFAB Center, University of Texas at Arlington, Texas 76019, USA*
[*]*wzhou@uta.edu*

Abstract: We report here a polarization-independent drop filter (PIDF) based on a photonic crystal self-collimation ring resonator (SCRR). Despite of the large birefringence associated with the polarization-dependent dispersion properties, we demonstrate a PIDF based on multiple-beam interference theory and polarization peak matching (PPM) technique. The PIDF performance was also investigated based on finite-difference time-domain (FDTD) technique, with excellent agreement between the theory and the simulation. For the designed drop wavelength of 1550 nm, the polarization-independent free spectral range is about 36.1 nm, which covers the whole optical communication C-band window. The proposed PIDFs are highly desirable for applications in photonic integrated circuits (PICs).

©2009 Optical Society of America

OCIS codes: (230.0230) Optical devices; (250.5300) Photonic integrated circuits; (130.3130) Integrated optics materials; (120.1680) Collimation; (999.9999) Photonic crystals.

References and links

1. H. Kosaka, T. Kawashima, A. Tomita, M. Notomi, T. Tamamura, T. Sato, and S. Kawakami, "Self-collimating phenomena in photonic crystals," Appl. Phys. Lett. **74**(9), 1212–1214 (1999).
2. J. Witzens, M. Loncar, and A. Scherer, "Self-Collimation in Planar Photonic Crystals," IEEE J. Sel. Top. Quantum Electron. **8**(6), 1246–1257 (2002).
3. L. Wu, M. Mazilu, and T. F. Krauss, "Beam Steering in Planar-Photonic Crystals: From Superprism to Supercollimator," J. Lightwave Technol. **21**(2), 561–566 (2003).
4. X. Yu, and S. Fan, "Bends and splitters for self-collimated beams in photonic crystals," Appl. Phys. Lett. **83**(16), 3251–3253 (2003).
5. P. T. Pakich, M. S. Dahlem, S. Tandon, M. Ibanescu, M. Soljacić, G. S. Petrich, J. D. Joannopoulos, L. A. Kolodziejski, and E. P. Ippen, "Achieving centimetre-scale supercollimation in a large-area two-dimensional photonic crystal," Nat. Mater. **5**(2), 93–96 (2006).
6. D. W. Prather, S. Shi, J. Murakowski, G. J. Schneider, A. Sharkawy, C. Chen, B. Miao, and R. Martin, "Self-collimation in photonic crystal structures: a new paradigm for applications and device development," J. Phys. D **40**(9), 2635–2651 (2007).
7. D. Zhao, C. Zhou, Q. Gong, and X. Jiang, "Lasing cavities and ultra-fast switch based on self-collimation of photonic crystal," J. Phys. D Appl. Phys. **41**(11), 15108–15112 (2008).
8. D. Zhao, J. Zhang, P. Yao, X. Jiang, and X. Chen, "Photonic crystal Mach-Zehnder interferometer based on self-collimation," Appl. Phys. Lett. **90**(23), 231114 (2007).
9. V. Zabelin, L. A. Dunbar, N. Le Thomas, R. Houdré, M. V. Kotlyar, L. O'Faolain, and T. F. Krauss, "Self-collimating photonic crystal polarization beam splitter," Opt. Lett. **32**(5), 530–532 (2007).
10. Y. Zhang, Y. Zhang, and B. Li, "Optical switches and logic gates based on self-collimated beams in two-dimensional photonic crystals," Opt. Express **15**(15), 9287–9292 (2007).
11. X. P. Shen, K. Han, F. Yuan, H. P. Li, Z. Y. Wang, and Q. Zhong, "New configuration of ring resonator in photonic crystal based on self-collimation," Chin. Phys. Lett. **25**(12), 4288–4291 (2008).
12. J. Hou, D. Gao, H. Wua, and Z. Zhou, "Polarization insensitive self-collimation waveguide in square lattice annular photonic crystals," Opt. Commun. **282**(15), 3172–3176 (2009).
13. P. Yeh, "Electromagnetic propagation in birefringent layered media," J. Opt. Soc. Am. **69**(5), 742–756 (1979).
14. B. E. A. Saleh, and M. C. Teich, "Fundamentals of Photonics," (A Wiley-Interscience publication, New York, 1991).

#114836 - $15.00 USD Received 27 Jul 2009; revised 7 Sep 2009; accepted 20 Sep 2009; published 16 Oct 2009
(C) 2009 OSA

1. Introduction

Self-collimation (SC) effect in photonic crystal (PC) structures allows diffractionless light propagation in perfect PCs without "physical" guiding boundaries (e.g. line-defect waveguide). It can also enable beam crossing without cross-talks [1, 2]. Various photonic devices based on this unique phenomenon have been theoretically and experimentally demonstrated including Fabry-Perot etalons, Mach-Zehnder interferometers, polarization beam splitters, photonic logic gates, and ring resonators, etc [3–11].

Typically, large birefringence exists in these SC based PC structures with high anisotropy, even though it is feasible to find a common self-collimation frequency range in some PCs that is shared by both TE and TM polarizations [12]. Here we present an ultra-compact polarization-independent drop filter (PIDF) design technique, based on self-collimation ring resonators (SCRRs) with large birefringence. Optical drop filters (ODFs) are one of the fundamental building blocks to construct many optical devices in optical communication systems. Many kinds of ODFs have been introduced based on optical fiber gratings, Fabry-Perot filters, waveguide micro-stripes, waveguide micro-disks and photonic crystal ring resonators. However, most ODFs reported to date are polarization dependent.

We propose a polarization peak matching (PPM) technique for efficient and effective design of PIDFs, based on the ring resonator operation principles and multiple-beam interference theory. This PPM technique, coupled with plane-wave expansion (PWE) and finite-difference time-domain (FDTD) techniques, offers a powerful tool for the design of such a new type of ultra-compact polarization-independent photonic filters, highly desirable for wavelength-division multiplexing (WDM) photonic integrated circuits and Si photonics.

In this paper, we first describe the PC dispersion properties in polarization-independent self-collimation frequency range, followed by the analysis of the SCRR operation characteristics based on the theory of multiple-beam interference. Finally, we present a "PPM" method for the design of PIDFs. The performance of this PIDF was also evaluated with FDTD technique, with excellent agreements between the theory and the simulation.

2. Design of polarization-independent drop filters

2.1. Polarization-independent self-collimation frequency range

A square lattice air hole based two-dimensional (2D) silicon photonic crystal (PC) structure is considered here, with the dielectric constant ε of 12.25 for Si. The ratio of the air hole radius r to the lattice constant a is 0.33. A portion of the simulated dispersion curves along ΓM direction is shown in Fig. 1(a), for both transverse-electric (TE) and transverse-magnetic (TM) polarizations, respectively. The equal frequency contours (EFCs), shown in Fig. 1(b) and Fig. 1(c), are EFCs in one fourth of the first Brillouin zone for TE and TM modes, respectively, all calculated by the plane-wave expansion (PWE) method. Although the real device structure, would, in practice, require 3D analysis, our 2D approach gives a general indication of the expected 3D behavior. This can offer us the design trade-offs and guidelines before the real structure design based on a completely 3D FDTD technique, which is typically computational time and memory consuming.

From Fig. 1(b) and Fig. 1(c), the EFCs in the frequency range between $0.17c/a$ and $0.19c/a$ for both TE and TM polarizations are close to straight lines normal to the ΓM direction (where c is the speed of light in vacuum). This indicates that both TE and TM lights in that frequency range can travel in the PC structure along ΓM direction, without any diffraction (so-called SC effect) [13]. This common SC frequency window for both TE and TM polarizations are essential in forming polarization-independent photonic devices based on SC effect. However, as shown in Fig. 1(a), the dispersion properties are different for these two polarizations, due to the birefringence nature in such 2D PC structures.

Within the SC frequency range of interest, i.e., between $0.17c/a$, and $0.19c/a$, both polarization modes have approximately linear dispersion relations, *i.e.*,

#114836 - $15.00 USD Received 27 Jul 2009; revised 7 Sep 2009; accepted 20 Sep 2009; published 16 Oct 2009
(C) 2009 OSA

$$f = (c / 2\pi n_e)k + f_0 \tag{1}$$

where n_e is the effective index for the SC beam, k is the Bloch wave-vector, and f_0 is the fitting parameter. Best linear fits can result in the following parameters: $n_{e,\mathrm{TE}} = 2.9737$, $f_{0,\mathrm{TE}} = 0.01905c / a$, and $n_{e,\mathrm{TM}} = 3.9217$, $f_{0,\mathrm{TM}} = 0.03804c / a$ for TE and TM polarizations, respectively. It is worth notice that significant birefringence exists with the ratio of the effective index for TE and TM modes to be close to 3 to 4 (i.e. $n_{e,TE}$:$n_{e,TM}$ = *3:4*), over SC frequency regime.

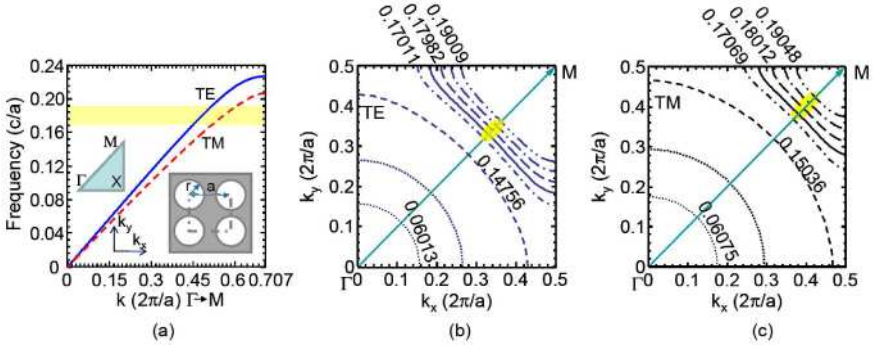

Fig. 1. (a) Square lattice air hole photonic crystal structure dispersion curves for two polarizations (TE and TM) along ΓM direction; Equal frequency contours (EFCs) of the first band for (b) TE modes and (c) TM modes. The air hole radius r equals 0.33a, where a is the lattice constant. The dielectric constant is assumed to be 12.25. The highlighted regions correspond to the SC frequency window.

2.2. Structure and characteristics of the self-collimation ring resonator (SCRR)

We show here the feasibility of a polarization-*independent* drop filter in such birefringent air hole PC structures, based on SC effect. The schematic of the proposed polarization-independent drop filters based on SC ring resonator (SCRR) structure is shown in Fig. 2(a), which consists of two beam splitters (BS1 and BS2) and two mirrors (M1, M2) [11]. Beam propagates in the SCRR employing self-collimation effect. As shown in the zoom-ins of Fig. 2(b), each mirror is formed by inserting an air bar along the ΓX direction, overlapping two and half rows of 18 air holes. Each beam splitter is a line defect formed by enlarging the radius of one-row of 19 air holes in the ΓX direction, from normal r = *0.33a*, to r_s = 0.4719a. The theoretical transmission (i.e., I_d/I_0) at drop port can be obtained based on the theory of multiple-beam interference in the following form [14]:

$$\frac{I_d}{I_0} = \frac{T_S^2}{(1-R_S R_M)^2} \cdot \frac{1}{1+[4R_S R_M / (1-R_S R_M)^2]\sin^2(\phi/2)} \tag{2}$$

where I_0 and I_d are the intensities of the input and the drop SC channels, R_S and T_S are the reflectivity and transmissivity of each splitter, R_M is the reflectivity of each mirror which is usually close to 100%. For lossless splitters and perfect mirrors, T_S = *1-*R_S and R_M = *100%*. ϕ is the phase delay after one loop beam propagation in the SCRR and can be expressed as

$$\phi = kl_e + \theta = k(l + l_p) + \theta \tag{3}$$

where k is the Bloch wave vector, θ is the total phase shift resulting from the phase discontinuities at two beam splitters and two mirrors, l_e is the effective propagation distance of one loop for SC light, l is the geometrical length of one loop, and l_p is the sum of the penetration depths at two mirrors. In general, θ and l_p are polarization dependent. From Eq. (2), when the phase delay ϕ is the integer multiples of 2π, the theoretical transmission at the

#114836 - $15.00 USD Received 27 Jul 2009; revised 7 Sep 2009; accepted 20 Sep 2009; published 16 Oct 2009
(C) 2009 OSA

drop port reaches the peak value, i.e. I_d=I_0 with R_M = *100%*, regardless of the beam splitter reflectivity values (R_S).

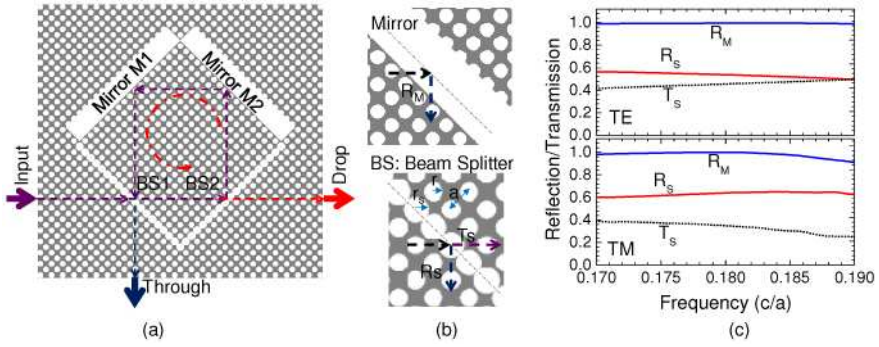

Fig. 2. (a) Schematic of polarization-independent drop filters based on self-collimation ring resonators (SCRRs) consisting of two beam splitters (BS1, BS2) and two mirrors (M1, M2); (b) Zoom-ins of the mirrors and beam splitters with key parameters defined; and (c) simulated reflection and transmission spectra for polarization-dependent mirrors and beam-splitters.

The performance of the mirrors and beam splitters was first evaluated based on 2D FDTD technique, with the results shown in Fig. 2(c). It is worth noting that there are large differences between TE and TM polarizations, in the simulated R_S and T_S values over SC frequency regime. To verify the theoretical analysis aforementioned, the numerical transmissions of the SCRR at the drop port for TE and TM modes are simulated with 2D FDTD technique. A Gaussian optical pulse is launched at the input port. The input power (I_0) and drop channel power (I_d) are monitored with two power monitors. The normalized drop channel transmission spectra (I_d/I_0) are plotted in Fig. 3 as solid blue lines, for $l = 37\sqrt{2}a$ and $l = 47\sqrt{2}a$, respectively.

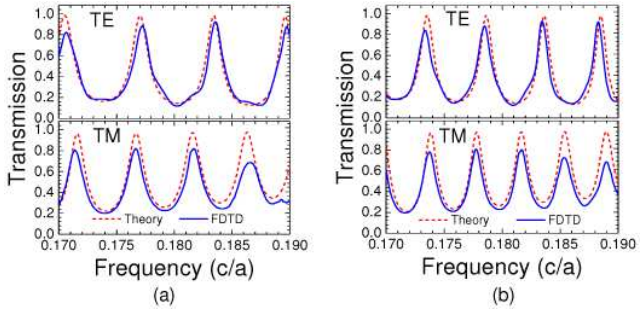

Fig. 3. Theoretical (dash lines) and FDTD simulated (solid lines) transmission spectra for the drop channel in the proposed SCRR based drop filters, with (a) $l = 37\sqrt{2}a$, and (b) $l = 47\sqrt{2}a$.

Based on our analysis reported earlier by Zhao *et al.* [8], the phase shift from one mirror reflection is equal to π. And the phase shift from one splitter reflection varies with the splitting ratio from π/2 to π. Therefore, the total phase shift θ value during one loop beam propagation should range between 3π and 4π. Although it is difficult to provide analytical θ and l_p values, we can obtain them based on the best fit of the numerically simulated FDTD transmission spectra with Eq. (2). Best fit results on the drop channel transmission spectra were obtained and shown in Fig. 3 for two arbitrarily chosen ring sizes, with $\theta_{TE} = 3.56\pi$ and $l_{p,TE} = 0.06\sqrt{2}a$ for TE polarization, $\theta_{TM} = 3.7\pi$ and $l_{p,TM} = 0.4\sqrt{2}a$ for TM polarization. Other parameters in Eq. (2) and Eq. (3) are based on the dispersion curve (k=$k(f)$) as shown in Fig. 1(a), and the reflection/transmission values (R_M, R_S, T_S) as shown in Fig. 2(c).

#114836 - $15.00 USD Received 27 Jul 2009; revised 7 Sep 2009; accepted 20 Sep 2009; published 16 Oct 2009
(C) 2009 OSA

The SCRR can work as a polarization-independent drop filter (PIDF) *only* if the peak drop frequencies for both TE and TM polarization modes coincide. Based on Fig. 3, the ratio of the free spectral ranges (FSRs) for TE and TM modes is about 4:3 for the same SCRR ring size, which agrees well with the ratio for the effective indices based on the dispersion properties shown in Fig. 1(a) ($n_{e,TE} : n_{e,TM} \approx 3:4$). Most importantly, the peak locations shift with the change of the geometrical ring size *l,* at different speeds for TE and TM modes. This opens up possibilities to match two polarization peaks at the same frequency with properly chosen SCRR ring size.

2.3. Design of polarization-independent drop filter (PIDF) based on SCRR

While it is possible to find the polarization peak matching (PPM) conditions by simply simulating all the transmission spectra for all possible ring sizes, here we propose an efficient approach to identify PPM conditions for different frequencies with different SCRR ring sizes.

Based on Eq. (2), maximum transmission (peak) occurs when the total phase delay after one loop beam propagation is $\phi_{TE} = 2j_{TE}\pi$ and $\phi_{TM} = 2j_{TM}\pi$, for TE and TM polarization modes, respectively, where j_{TE} and j_{TM} are positive integers. Under this condition, Eq. (3) can be expressed as the following:

$$2j_{TE}\pi = k_{TE}(l + l_{p,TE}) + \theta_{TE}, \quad 2j_{TM}\pi = k_{TM}(l + l_{p,TM}) + \theta_{TM} \tag{4}$$

where $k = k(f)$ as shown in Fig. 1(a). Theoretically, we can derive the peak locations f_{pk} for each SCRR loop size *l*, where $l = 35, 37, 39, \cdots, 55(\sqrt{2}a)$. The results are shown in Fig. 4 (a) and (b), with peak frequency values shown as blue circles and red dots for TE and TM polarizations, respectively. Notice that the slopes (solid lines) for each integer values of j_{TE} and j_{TM} are different, due to the existing birefringence and different polarization-dependent fitting parameters. This indeed is essential in obtaining the PPM matching conditions, in birefringent PC structures.

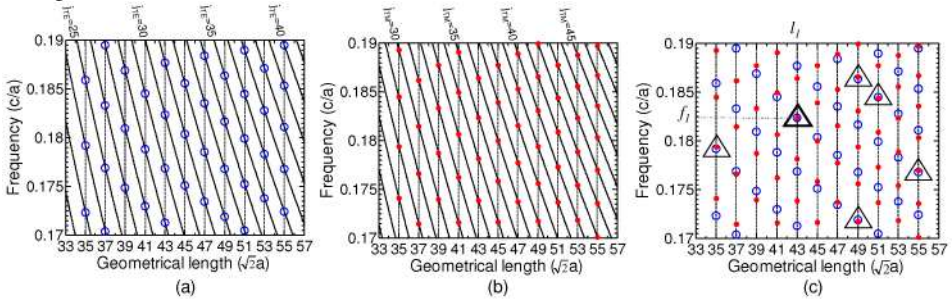

Fig. 4. Theoretically calculated peak frequencies shown in blue circles and red dots for (a) TE and (b) TM polarizations, respectively, at each geometrical length (SCRR size) *l*. The corresponding integer values j_{TE} and j_{TM} are also shown. (c) Polarization peak matching (PPM) map with triangles identifying polarization independent operation conditions where TE (blue circles) and TM (red dots) peaks overlap.

Plotting these peak frequency values together for both TE and TM polarizations, we can obtain the PPM map, as shown in Fig. 4(c), where PPM conditions can be obtained by identifying the overlap locations, highlighted with "triangle" symbols. A perfect overlap between TE (blue circles) and TM (red dots) polarizations in the PPM map indicates peak drop efficiencies at the same frequency for both polarization modes. In practical application, many design options are acceptable, with certain design tolerance window for PIDFs. There are at least six acceptable design options, shown as "triangle" symbols in Fig. 4(c), with one of them showing almost a perfect design ($l_1 = 43\sqrt{2}a$, f_1 = *0.1824 c/a*). The results suggest

#114836 - $15.00 USD Received 27 Jul 2009; revised 7 Sep 2009; accepted 20 Sep 2009; published 16 Oct 2009
(C) 2009 OSA

that polarization independent filters are feasible, for any design frequencies, by properly choosing the right size of the SCRRs and the lattice parameters.

To validate this theoretical prediction, we simulated transmission spectra for a few different SCRR sizes *l*, based on FDTD technique. Shown in Fig. 5(a) are transmission spectra for the SCRR loop size $l_1 = 43\sqrt{2}a$. We can find both TE and TM polarization modes peak at f_1*=0.1824 c/a*. This agrees extremely well with the results shown in Fig. 4(c). The corresponding propagating fields were also simulated and shown in Fig. 5(b), for both TE and TM polarizations at this design frequency. The frequency-selectivity of the filter is evident based on the simulated transmission spectra shown in Fig. 5(a). Another set of propagating field plots is also shown in Fig. 5(c), for a through channel at frequency f_1 *= 0.1800 c/a*. Such a polarization-independent drop filter can be designed to operate at any frequencies, by simply choosing the right lattice parameters. For an operating wavelength of 1550 nm, the lattice constant *a* and air hole radius *r* can be chosen to be 282.7nm and 93.3nm, respectively. The polarization-independent free spectral range (FSR) is equal to 36.1nm, which covers the whole optical communication C-band window.

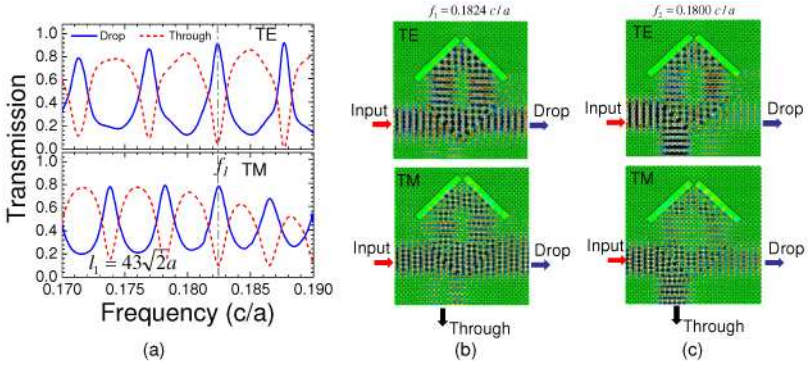

Fig. 5. (a) FDTD simulated drop channel transmission (solid blue lines) and through channel output (dash red lines) for both TE and TM polarizations at SCRR loop size $l_1 = 43\sqrt{2}a$. Notice PPM occurs at f_1 *= 0.1824 c/a*, which agrees very well with the results shown in Fig. 4(c) based on the theoretical calculations. (b, c) FDTD simulated magnetic-field distribution for TE polarization (top) and electric-field distribution for TM polarization (bottom) at (b) matching condition f_1 *= 0.1824 c/a* for drop channel, and (c) f_2 *= 0.1800 c/a* for through channel.

3. Conclusion

In conclusion, we propose a polarization-independent drop filter based on the self-collimation ring resonator in a hole-type silicon photonic crystal. Based on polarization peak matching (PPM) method, we can efficiently design polarization-independent drop filters, operating at any frequencies. The designed filter performance was also evaluated based on FDTD simulation technique, with excellent agreements between the simulation and the theory. For the operating wavelength at 1550nm, the polarization-independent FSR is equal to 36.1nm, covering the whole optical communication C-band window. This ultra-compact polarization-independent drop filter is highly desirable for wavelength-division multiplexing (WDM) based photonic integrated circuits.

Acknowledgments

This work was supported in part by the Natural Science Foundation of Fujian Province of China under Grant No.2009J01012 and No.2009J05140, by the Program for the Key Teacher in University by the Ministry of Education of China (No. NCET-04-0615), and by US AFOSR MURI program (No. FA9550-08-1-0337).

#114836 - $15.00 USD Received 27 Jul 2009; revised 7 Sep 2009; accepted 20 Sep 2009; published 16 Oct 2009

(C) 2009 OSA